Results in Physics 55 (2023) 107185

Contents lists available at ScienceDirect

Results in Physics

journal homepage: www.elsevier.com/locate/rinp

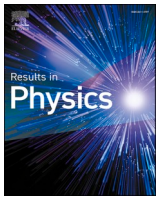

The computational study of external heat flux and silicon doping effect on displacement of C_{20} molecule in a carbon nanotube (CNT): A molecular dynamics method

Xinwei Guo [a,b,*], S. Mohammad Sajadi [c], Nafis Ahmad [d], Tariq J. Al-Musawi [e], Navid Nasajpour-Esfahani [f], Sh. Esmaeili [g], M. Abdulfadhil Gatea [h,i], Ali Alsalamy [j], D. Toghraie [k]

[a] Ural Institute, North China University of Water Resource and Electric Power, Zhengzhou, Henan 450045, China
[b] Institute of Thermal Energy Engineering, School of Mechanical Engineering, Shanghai Jiao Tong University, Shanghai 200240, China
[c] Department of Nutrition, Cihan University-Erbil, Kurdistan Region, Iraq
[d] Department of Physics, College of Science, King Khalid University, P.O. Box: 960, Abha 61421, Saudi Arabia
[e] Building and Construction Techniques Engineering Department, Al-Mustaqbal University College, 51001 Hillah, Babylon, Iraq
[f] Department of Materials Science and Engineering, Georgia Institute of Technology, Atlanta 30332, USA
[g] Faculty of Physics, Semnan University, P.O. Box: 35195-363, Semnan, Iran
[h] Technical Engineering Department College of Technical Engineering, The Islamic University, Najaf, Iraq
[i] Department of Physics, College of Science, University of Kufa, Iraq
[j] College of Technical Engineering, Imam Ja'afar Al-Sadiq University, Al-Muthanna 66002, Iraq
[k] Department of Mechanical Engineering, Khomeinishahr Branch, Islamic Azad University, Khomeinishahr, Iran

ARTICLE INFO

Keywords:
Heat flux
Silicon doping
C_{20} molecule
Molecular dynamics method

ABSTRACT

This study focuses on the behavior of the Carbon Nanotube (CNT)-C_{20} system as a nano-pumping configuration for drug delivery processes. The system was modeled using a molecular dynamics (MD) method, and the effects of external heat flux and silicon doping were investigated. The predicted MD outputs showed high stability throughout the nanopumping process, even when different ratios of external heat flux were applied. The entropy value of the CNT-C_{20} system decreases from 412.91 to 403.394 eV/K as the heat flux increases to 0.03 W/m^2. Also, the kinetic energy of the target atomic sample increased from 3.50 to 5.42 eV as heat flux increased. This kinetic energy enlarging occurred for the translational component of the target molecule's kinetic energy, and the rotational component didn't change effectively. Additionally, the results show that increasing atomic doping of silicon particles from 1 to 3 % decreased the displacement time of C_{20} molecule (7.22 ps for a 3 % doping ratio), indicating that atomic doping may also improve the nano-pumping process. By increasing Si doping to 3 %, the potential energy decreased, and the stability of the defined compound was reduced. This procedure caused the target molecule to not stabilize inside the nanotube sample, and this molecule displaced inside the deliverer system in less time. However, the negative ratio of potential energy showed physical stability of the total system wasn't disrupted. With further doping increase to 5 %, the defined compound's potential energy increased and stability enlarged. This process can be delayed nano-pumping procedure. Overall, the outcomes of this simulation provide insights into the optimal method for pumping fluids at the nanoscale and for drug delivery systems. These findings have practical implications for developing more efficient and effective drug delivery technologies that can help improve patient outcomes.

Introduction

In 1992, two researchers in NEC's basic research laboratory worked on the macroscopic production of carbon nanotubes (CNTs) [1,2]. In this production process, CNT is created by folding or rolling two-dimensional graphite into a hollow cylindrical structure with a nanometer diameter [3,4]. CNT has unique properties that make them very important from an economic point of view. These structures are hard; they are as hard as a diamond (the hardest natural substance in nature). These structures have a low gravitational weight, and their density is a

* Corresponding author.
E-mail address: gxwwos@126.com (X. Guo).

https://doi.org/10.1016/j.rinp.2023.107185
Received 29 June 2023; Received in revised form 11 October 2023; Accepted 11 November 2023
Available online 13 November 2023

quarter of steel's, while CNTs are ten times stronger than steel [5]. CNT has a high heat capacity, which is generally 20 times stronger than steel. They have good thermal conductivity [6,7] and have good electrical conductivity [8,9]. On the other hand, these nanotubes are chemically neutral. Therefore, they are chemically stable, which makes CNT resistant to corrosion [10]. Today, CNTs can be used as a tissue scaffold for nerve cells. Moreover, in the medical field, it can treat brain injury, drugs delivered to damaged cells, destroy cancerous tumours, and gene therapy [11]. As drug carriers, these nanotubes can target certain cancer cells, destroy cancer cells using a lower dose of drugs, and avoid damaging healthy cells.

Many studies were conducted on various CNT applications [12]. Based on DFT theory, and using hydroxyl and carboxyl functionality, Karimzadeh et al. [13] studied the interaction and binding properties of anticancer drug doxorubicin (DOX) with single-walled carbon nanotubes (SWCNT). This study showed that the adsorption energy between CNT and DOX in the gas phase was higher than in other phases and, the functionalization of SWCNT increased absorption power, and stability of DOX. Naderi et al. [14] studied the effect of adding CNT on change in temperature, total energy, atomic density, atomic velocity and atomic temperature of H_2O (as base fluid) using molecular dynamics simulation (MDS). This study's results indicate that by adding 4 % of CNT nanoparticles to the base fluid, the atomic density, velocity, and temperature reached their maximum values of 0.058 atom/Å^3, 0.067 Å/ps and 1205 K, respectively. Vahedi et al. [15] created multi-scale modelling to study heat transfer along with CNT/epoxy nanocomposites using a combined finite element method (FEM) and MD. This study showed that increasing the diameter of CNT fillers caused an increase in the effect of surface thermal resistance, which increased thermal conductivity. Safaei et al. [16] examined the effect of the type of chirality, and the number of CNT walls on carbon NT mechanical properties. The results show that by changing the number of CNT, critical axial buckling strain significantly changed. Ranke et al. [17] examined the interactions of CNTs with different anticancer drugs using MDS. The results show that the diameter of CNTs had a significant effect on the movement and encapsulation of the drug. CNTs with a diameter of 20.3 Å had the most optimal state in this study. Karimzadeh et al. [18] examined ethanol molecules on the processes of the encapsulation of drug molecules in CNTs. The results show that the presence of ethanol molecules led to a reduction in the encapsulation of drug molecules. Pakdel et al. [19] investigated the interaction of the anticancer agent doxorubicin with SWCNT with different diameters using MDS. This study showed that targeted drug delivery of DOX using SWCNT failed in the presence of nicotine molecules. Because the presence of nicotine molecule caused more force to be needed to pull the drug out of CNT, this process took longer. Zhou et al. [20] examined the effect of electric field (EF) and vacancy defect on nano-pumping performance of boron-nitride nanotube (BNNT) using MDS. The results revealed that the EF implementation inside the MD box improves the nano-pumping performance of the BNNT structure. Xie et al. examined the [21] examined the performance of CNT as a nanopump sample for drug delivery systems, using MDS and external heat flux/electric field effects. The results reveals that increasing the heat flux amplitude ratio, the displacement time of C_{20} molecule decreased, and the nano-pumping process to occur in a smaller time. Weidong et al. [22] examined the displacement of the C_{20} molecule in the presence of different EF and silicon (Si) doping on CNT using MDS. The results revales that increasing the EF causes translational displacement of the target molecule, and the nano-pumping process is done in a shorter MD time. However, Si doping increases the displacement time of C_{20} molecules. Sabetvand et al. [23] examined the BNNT performance for drug delivery applications using MD simulation. In the present study, the optimized for the nano-pumping time was 7.79 ps. This study showed that MDS the nanopumping process well.

By combining three commonly used platforms, including hydrogels, liposomes and SWCNT, Madani et al. [24] developed an externally controllable drug delivery system. This new structure, called carbon nanotube-liposome (CLC), is loaded with a model drug (FITC-Dex). This study's results show that Amdel drug (FITC-Dex) could be stored for several days. Also, the stimulation time can be changed to modify the amount of drugs released. For this purpose, a NIR laser was used in the hydrogel scaffold.

Previous studies show that MDS can well calculate the atomic behavioral, mechanical and thermal properties of various nanostructures [25–27], including carbon nanostructures [28]. On the other hand, the present study focuses on developing a breakthrough nano-pumping technology for drug delivery systems using the Carbon Nanotube (CNT)-C_{20} system as a nano-pumping configuration using MDS. Compared to other papers, this study specifically focuses on the behavior of the Carbon Nanotube (CNT)-C_{20} system as a nano-pumping configuration. This study's unique aspect is utilizing an MD method to investigate the atomic development of the modeled samples in the presence of an external heat flux and silicon doping. On the other hand, recent study indicated that the MDS would be able to compute the nano-pump process in CNTs well, much as the experimental method [29]. By exploring the effects of external heat flux and atomic doping on the nano-pumping process, this research aims to enhance the understanding of fluid pumping at the nanoscale. Furthermore, present study emphasizes the stability of the CNT-C_{20} system throughout the nanopumping process. The results demonstrate that the nano-pumping system remains intact even with varying ratios of external heat flux and different percentages of silicon doping. For this purpose, an external heat flux's effect with magnitude of 0.01, 0.02, 0 and 0.03 W/m^2 and silicon doping with the percentages of 1, 2, 3, 4, and 5 % were added to the CNT. The motivation behind present manuscript is to provide valuable insights into optimizing fluid pumping at the nanoscale and improving drug delivery systems. By focusing on the specific nano-pumping configuration and exploring the effects of external heat flux and atomic doping, this research advances nanoscale pumping technologies and their applications in drug delivery.

Simulation

MDS

MDS is a computational method that can analyze the atomic and molecular motions. During a specific time period, atoms and molecules have the opportunity to interact in this method. In addition, in this method, microscopic results determined the macroscopic properties of the system. In MDS, Newton's equation of motion is numerically solved to determine the trajectories of atoms and molecules. Because the simulated molecular structure has an unlimited number of component particles, the numerical equation is applied. There is no other approach that can be used to examine such complex systems than numerical methods. The equation of Newton's second law is as follows [30]:

$$\boldsymbol{F} = m\boldsymbol{a} = m\frac{d\boldsymbol{v}}{dt} = m\frac{d^2\boldsymbol{r}}{dt^2} \tag{1}$$

In Eq. (1), **F** is the applied force to each atom, m is the mass, and **a** and **r** are the acceleration and position of each atom, respectively. The created movement in the particles has changed the position of the particles from their initial state, which will affect how the charge was applied to the particles. Finally, this particle displacement rate was determined in MDS using the velocity-Verlet algorithm, a common integral method. The velocity-Verlet algorithm is as follows [30–32]:

$$r(t+\Delta t) = r(t) + \Delta t\ v(t) + \frac{\Delta t^2 a\ (t)}{2} \tag{2}$$

$$v(t+\Delta t) = v(t) + \Delta t\ v(t) + \frac{\Delta t\ (a\ (t) + a(t+\Delta t)\ )}{2} \tag{3}$$

On the other hand, the force can be obtained via the potential energy

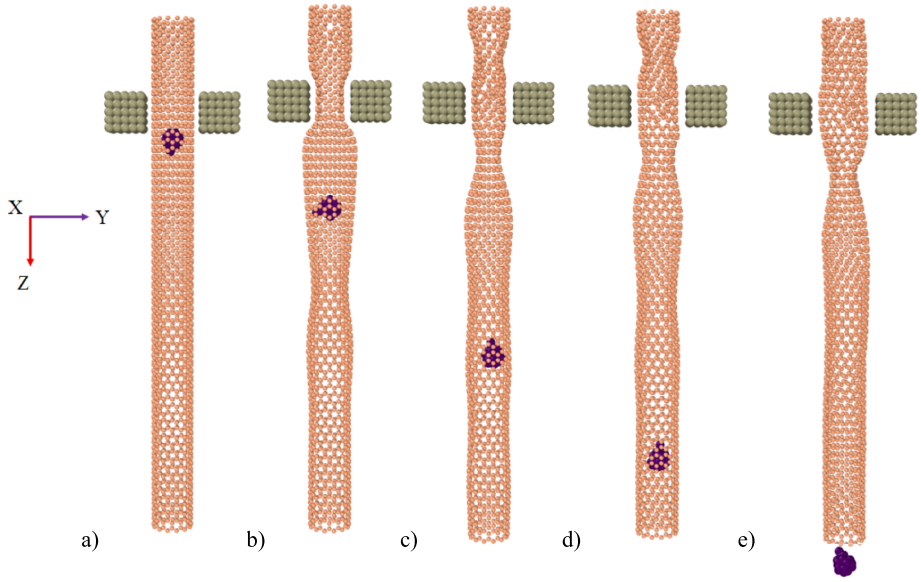

Fig. 1. A view of the nano-pumping process in CNT at: a) 0, b) 2.5, c) 4.5, d) 6.5, and e) 8.5 ps.

gradient equation, except that in this equation, in addition to the position of each atom, potential energy is a determining factor. This equation is given below:

$$F = -\frac{dU(r)}{dr} \tag{4}$$

At this stage, the particles making up the structure are hit with a force that is directly related to their spatial relationship to one another. For some time, these particles will be affected by this force, which is considered to be constant. In most cases, defining a potential function or describing expressions that pertain to the interactions of system components is necessary for the MDS. In fact, the potential function defines the simulated system, and consequently, a complete description of interatomic interactions appears. To be more precise, the MD simulated structure consists of infinite particles, each of which exerts a force on each other, so determining the interatomic interactions requires a mathematical function. This study uses Tresoff and Lennard Jones (LJ) potentials to characterize the atomic development of modeled samples in the presence of an external heat flux. The Tersoff potential is commonly used to describe the bond formation and breaking in covalently bonded materials such as CNTs, while the LJ potential is used to describe the non-bonded interactions between atoms. [33–35]. Tersoff potential function is represented as follow as follows [36]:

$$E = \frac{1}{2}\sum_{i}\sum_{j\neq i} U_{ij} \tag{5}$$

$$U_{ij} = f_C(r_{ij})\left[a_{ij}f_R(r_{ij}) + b_{ij}f_A(r_{ij})\right] \tag{6}$$

which consists of three terms f_R (absorbent interaction), f_A (repellent interaction), and $f_c(r)$. The Tersoff potential is a multi-body potential that takes into account the coordination and angular dependence of bond formation and breaking. It has been widely used in molecular dynamics simulations of carbon nanotubes and other covalent materials due to its accuracy and ability to capture the complex bond formation and breaking processes. The LJ potential, on the other hand, is a pairwise potential that describes the non-bonded interactions between atoms. It is commonly used to describe van der Waals interactions and short-range repulsive interactions between atoms. The LJ potential function is given below [35]:

Table 1
The simulation settings in current computational work.

Simulation Parameter	Parameter Setting
Computational Box Length	60 × 80 × 210 Å^3
Boundary Condition	Periodic Boundary Condition
Thermostat	Nose-Hoover
Initial Temperature	300 K
Ensembles	NVT/NVE
Time Step	0.001 ps
Damping Ratio for Temperature	0.001
Simulation Time	9 ps

$$U_{LJ} = 4\varepsilon\left[\left(\frac{\sigma}{r}\right)^{12} - \left(\frac{\sigma}{r}\right)^{6}\right] \tag{7}$$

The values of σ and ε are calculated as follows [37,38]:

$$\varepsilon_{ij} = \sqrt{\varepsilon_i \varepsilon_j} \tag{8}$$

$$\sigma_{ij} = \frac{\sigma_i + \sigma_j}{2} \tag{9}$$

By using both Tersoff and LJ potentials in our simulations, we aimed to accurately capture the complex atomic interactions in the CNT-C_{20} system and investigate the effects of external heat flux and silicon doping on the nano-pumping process.

Simulation details

At the most fundamental level of simulation systems, a structure was structurally modeled using a variety of software. The CNT with a diameter and length of 10 and 134 Å were modelled by VMD software, and packed with C_{20} molecule with Packmol software. Two copper Tips are produced in the Y direction to produce oscillation in the NT. The structure's starting temperature was set at 300 K, and it was managed by a Nose-Hoover thermostat. All three directions had periodic boundary conditions. The number of simulated particles was 101,338 atoms. NVT ensemble was used in the present study. The simulation time was 9 ps. The simulated structure is schematically shown in Fig. 1. Our simulation details in current computational research listed in Table 1.

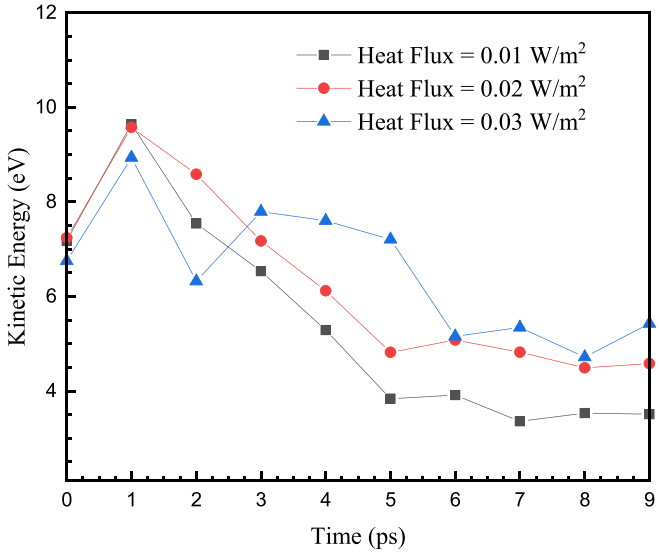

Fig. 2. The kinetic energy changes at different external heat fluxes.

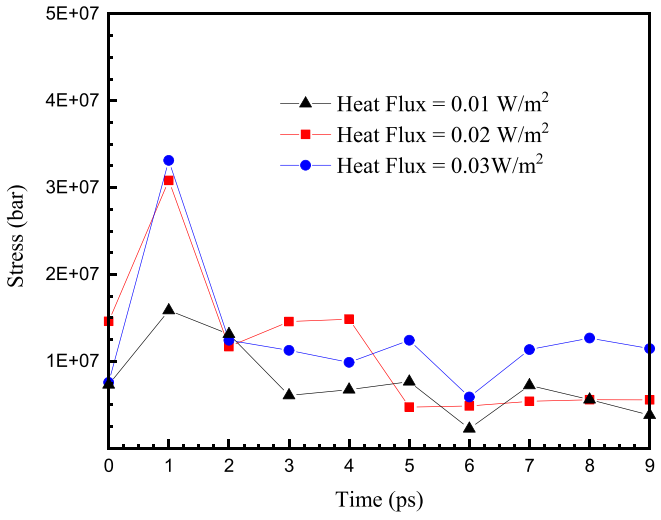

Fig. 3. The stress changes at different external heat fluxes.

Results and discussion

In general, drug delivery is a process for managing pharmaceutical compounds to achieve therapeutic effects in the human or animal body. Targeted drug delivery system by nano method includes delivering the drug at a certain time and with a controlled dose to achieve specific drug goals. It is significantly safer and more effective than the classical drug delivery methods. Therefore, this paper studied the displacement time of C_{20} molecule, kinetic energy, stress on the structure, potential energy and entropy in the simulated CNT.

Magnitude of external heat flux

To begin, it was noted that the external heat flow had an effect on the nano-pumping process. To apply an external heat flux, a heat source and a heat sink were each specified on both sides of the CNT. MD outputs are predicted by external heat flux increasing, the nano-pumping time decreasing. This procedure shows nano-pumping process effectively occurs in larger heat fluxes. This atomistic evolution arose from mechanical wave enlarging inside NT by heat flux increasing. The displacement time of C_{20} molecule was estimated to check the optimum

Table 2
The change in kinetic energy and stress of structures at different external heat fluxes.

The magnitude of external heat flux	Kinetic energy (eV)	Stress (10^6 bar)
0.01 (W/m^2)	3.5079 (±0.677)	3.8065 (±1.243)
0.02 (W/m^2)	4.5799 (±0.207)	5.5565 (±2.492)
0.03 (W/m^2)	5.4247 (±0.473)	11.457 (±2.556)

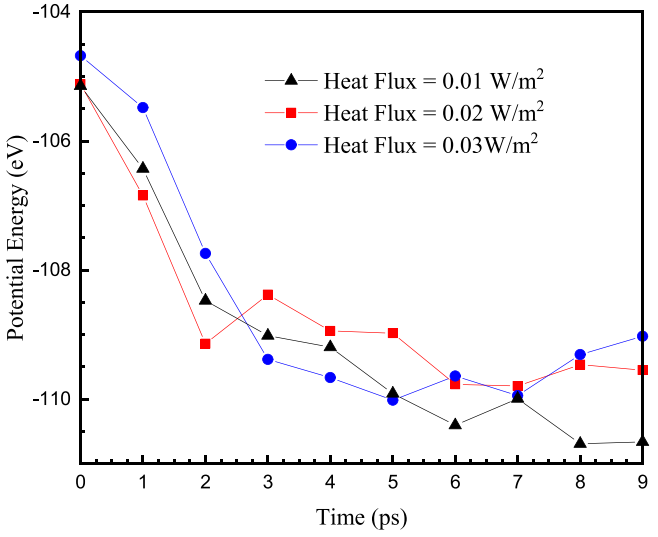

Fig. 4. The potential energy changes at different external heat fluxes.

state for the nano-pumping process. Physically, described improvement arose from effective collision number increasing among NT particles by implementing external heat flux to them. Furthermore, these effective collision didn't distrupt the stability of deliverer system and designed system can be used in actual cases. The kinetic energy of C_{20} molecule was another parameter described in this improvement procedure. As shown in Fig. 2, the kinetic energy of target atomic sample increased as heat flux increasing. This kinetic energy enlarging occurred for translational component of target molecule's kinetic energy and rotational component of them didn't changes effectively. So, it was concluded that C_{20} molecule mobility enlarged in the nano-pumping mechanism by defining external heat flux. Previous studies also show that increasing the heat flux leads to an increase in the kinetic energy of the target molecule in the nanotube [21]. Also, this effective molecular displacement arose from lattice stress implemented to fullerene samples in our simulations. Physically, by increasing the stress ratio inside the NT, more lattice force in the displacement direction was implemented in C_{20} molecule (See Fig. 3 and Table 2).

The potential energy variation can show more details about heat flux's effect on CNT-based samples' nano-pumping performance. Simulation outputs indicated potential energy ratio decreases as heat flux increases. So, we concluded that the atomic attraction force between CNT and C_{20} samples decreased and the displacing of target molecules was effectively occurred. Furthermore, negative ratio of atomic systems potential energy showed physical stability of them in the presence of external heat flux. So, we expected mean distance among various particles in NT didn't diverge by simulation time passing and inappropriate phenomena, such as twisting of the deliverer system did not occur in defined condition (See Fig. 4).

In the modeled nano-pump system, the entropy parameter analysis of specified molecules may be thought of as physical stability. To calculate the entropy using LAMMPS, it can use the compute enthalpy/entropy command [39]. This command computes the enthalpy and entropy of a group of atoms based on their positions and velocities. This parameter for atom i is computed using the following formula in LAMMPS:

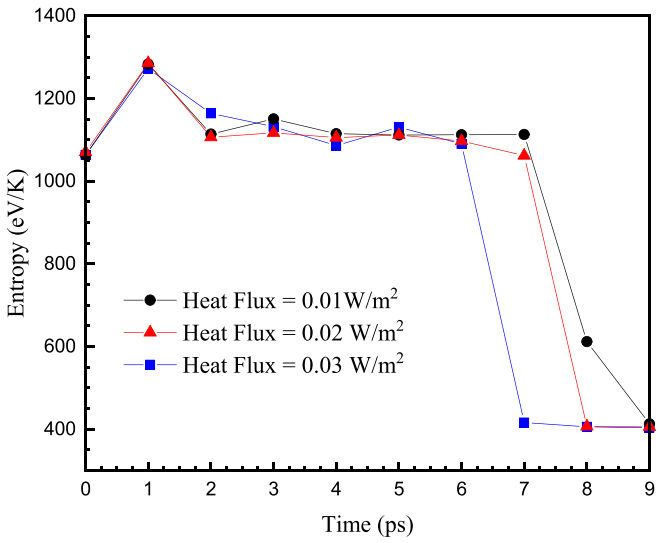

Fig. 5. The entropy changes at different external heat fluxes.

Table 3
The change in potential energy and entropy at different external heat fluxes.

The magnitude of external heat flux	Potential energy (eV)	Entropy (eV/K)
0.01 W/m^2	−110.66 (±0.352)	412.9166 (±5.514)
0.02 W/m^2	−109.551 (±0.404)	405.8290 (±3.481)
0.03 W/m^2	−109.025 (±0.165)	403.3944 (±1.729)

$$S = -2\pi\rho k_B \int_0^{r_m} [g(r)\ln g(r) - g(r) + 1] r^2 dr \quad (10)$$

where r is a distance, g(r) is the radial distribution function of atom i, and ρ is the density of the system.

Therefore, this parameter ratio determined in this research part as a function of external heat flux. Numerically, this parameter value reached 403.3944 (±1.729) eV/K by implementing heat flux with 0.03 W/m^2 magnitude (see Fig. 5). Our results in this section showed the entropy of CNT-C_{20} system decreased by heat flux increasing. So, we may conclude that changing the heat flux setting in different ratios had no effect on the nanopumping system. However, the nano-pumping mechanism only appears in a few heat fluxes, and this behavior should be anticipated for actual applications. The numerical results are reported in Table 3.

The effect of Si doping percentage in optimized heat flux

Next, the effect of Si doping on atoms' evolution in the nano-pumping process was reported. MD method introduced atomic doping as an effective parameter for target molecule displacement inside CNT. For this purpose, silicon particles with the percentages of 1, 2, 3, 4, and 5 % were doped to CNT. Fig. 6 represents a schematic of simulated nanostructures. Furthermore, by increasing doping up to 4 and 5 %, the duration of nanostructure displacement increased. Numerically, by

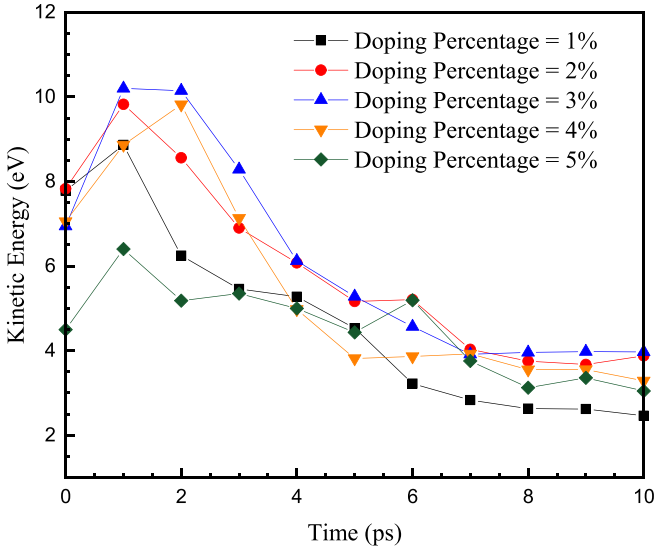

Fig. 7. The kinetic energy changes at different doping percentages.

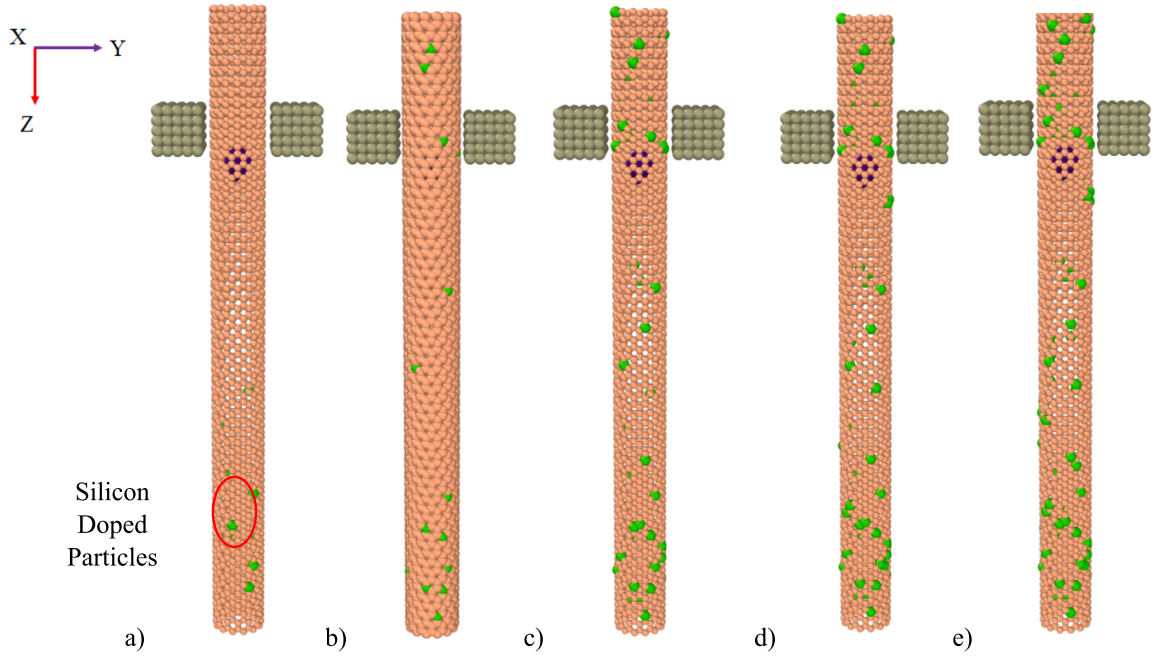

Fig. 6. A view of CNT in the presence of a) 1%, b) 2%, c) 3%, d) 4%, and e) 5% Si doping.

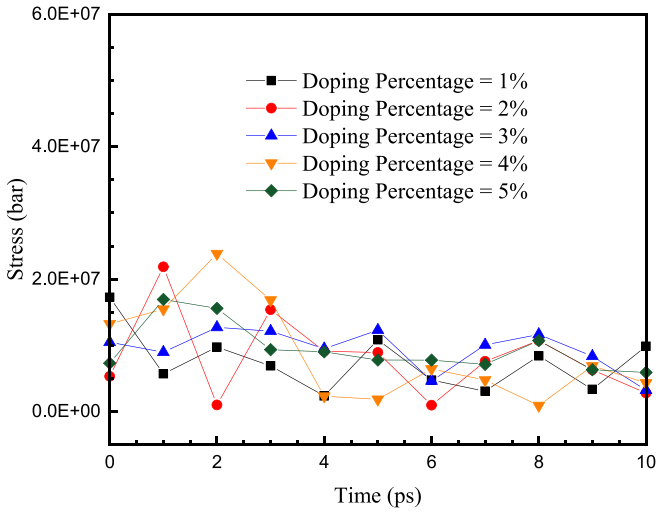

Fig. 8. The stress changes at different doping percentages.

Table 4
The change in kinetic energy and stress of structures at different doping percentages.

Doping percentages (%)	Kinetic energy (eV)	Stress (10^6 bar)
1	2.4614 (±0.522)	9.867 (±4.912)
2	3.8776 (±0.214)	2.794 (±4.646)
3	3.9730 (±0.541)	3.224 (±3.216)
4	3.2888 (±0.322)	4.329 (±2.085)
5	3.0492 (±0.778)	5.9034 (±4.697)

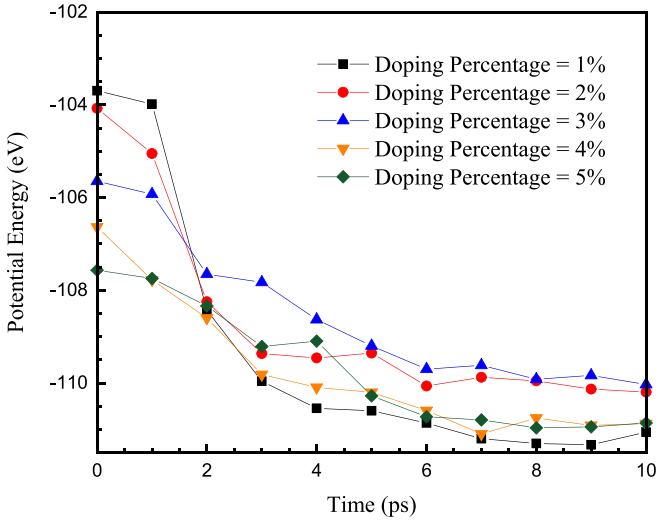

Fig. 9. The potential energy changes at different doping percentages.

increasing doping to 4 and 5 %, the duration of C_{20} molecule displacement increased to 8.53 and 8.88 ps. With a further increase in doping 6 % and above), nano-pumping process was disrupted, and C_{20} molecule did not exit from the CNT. But, by increasing doping up to 5 %, Si particles disturb the pumping process and prolong its time. Also, previous studies show that that this range time (7 to 12 ps) is enough for the target molecule displacement from the nanostructure [21,22].

The kinetic energy of defined compounds is reported in Fig. 7 for this purpose. Computationally, Si doping (up to 3 %) in the pristine sample caused nano-pumping time to decrease, and C_{20} molecule exit from improved NT in a shorter time (7.22 ps for a 3 % doping ratio). This

Table 5
The change in potential energy and entropy of structures at different doping percentages.

Doping percentages (%)	Potential energy (eV)	Entropy (eV/K)
1	−111.0633 (±0.873)	408.032 (±3.586)
2	−110.1961 (±0.782)	400.077 (±2.832)
3	−110.0331 (±0.727)	395.439 (±2.454)
4	−110.7678 (±0.531)	406.377 (±3.847)
5	−110.8627 (±0.928)	408.983 (±3.536)

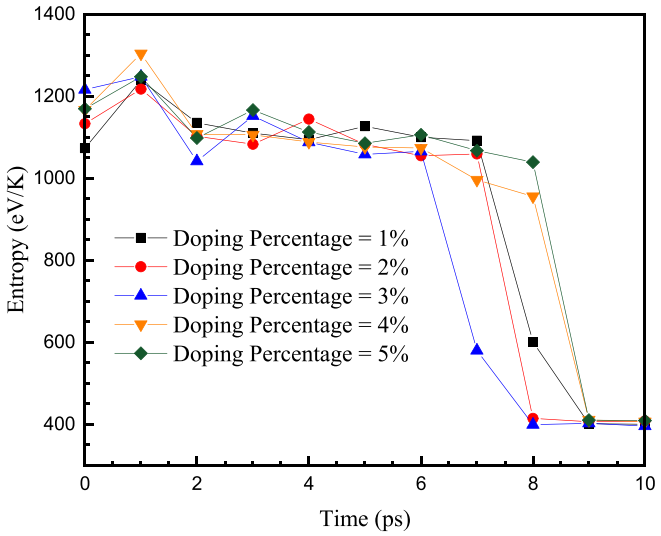

Fig. 10. The entropy changes at different doping percentages.

process arose from kinetic energy increasing inside the MD box. As shown in Fig. 7, kinetic parameter reached 3.9730 (±0.541) eV by a 3 % doping ratio inserting to pristine CNT. But, with the further increase of doping up to 5 %, silica particles led to disturbance in pumping process and kinetic energy decreased to 3.0492 (±0.778) eV. So, we expect needed energy to produce effective displacement in target sample decreased by doping process implementing to pristine atomic NT. This improvement maximized using 3 % doping in modeled sample. *Generally, an excessive increase in doping can disrupt the nanopumping process inside the nanotube* [40].

This part calculated the change in the stress parameters as a function of time. Fig. 8 shows that the stress parameter decreased by atomic doping implementation (to 3 %), and this process caused the C_{20} molecule to be pushed with a lesser atomic force. Finally, by increasing doping up to 5 %, the stress on the lattice increased. Numerically, the stress of CNT-C_{20} system converged to 5.9034 (±4.697) × 10^6 bar (with 5 % doping). The results are listed in Table 4.

This part calculated potential energy as a function of time. Fig. 9 shows potential energy changes in this step. By increasing Si doping to 3 %, the potential energy decreased and the stability of defined compound reduced. This procedure caused target molecule didn't stabilize inside NT sample, and this molecule displaced inside deliverer system in lesser time. But, negative ratio of potential energy showed physical stability of total system didn't disrupt. With further doping increase to 5 %, the defined compound's potential energy increased and stability enlarged. This process can be delayed nano-pumping procedure. Potential energy converged to −110.8627 (±0.928) eV with 5 % Si doping (Table 5). We concluded that the modification procedure enhances the stability of the nano-pump system (CNT-C_{20} system). To enhance the efficacy of CNT-C_{20} nano-pumping for medical applications, we introduced this mechanism by introducing external heat flux.

In the final section of our computational research, the entropy of

defined compounds is reported in Fig. 10 for this purpose. Structurally, this atomic evolution (doping up to 3 %) decreased the entropy of defined sample. With a further increase in doping to 5 %, the entropy of defined sample increased. Numerically, entropy decreased to 395.439 (±2.454) eV/K by implementing 3 % doping to the modelled NT and increased to 408.983 (±3.536) eV/K by a further increase of Si doping. The entropy decreasing in the presence of 3 % doping in modeled NT indicated the optimum movement of deliverer system to transfer the target molecule. Structurally, we can say the effective displacement of NT occurred in Z direction and atomic fluctuations in Y and Z directions minimized in presence of 3 % atomic doping.

Conclusion

In our most recent computational study, we discussed the effects of Si doping and external heat flux on the nano-pumping of the Carbon Nanotube (CNT) sample. Molecular Dynamics (MD) method was used for this. Technically, the displacement of C20 molecule within the NT was recorded for the study of nanopumping process. Important outputs from our MD simulations can be reported as below items:

- CNT-C_{20} system has physical stability. This behavior arose from appropriate MD settings in our simulations.
- Nanopumping process time decreased to 6.96 ps by increasing heat flux to 0.03 W/m^2. Moreover, nano-pumping process time increased to 8.88 ps, increasing Si doping to 5 %.
- By increasing external heat flux, the nano-pumping process improvement arose from C_{20} molecule's kinetic energy increasing and more mobility of this target sample inside the MD box, which arose from more lattice stress on C_{20} molecule.
- The potential energy converged to −110.8627 (±0.928) eV with 5 % Si. So, doping process improved the stability of nano- pumping system (CNT-C_{20} system).

From these outputs, we concluded Si doping with an optimized ratio could be introduced as an effective mechanism to improve the nano-pumping stability of CNT sample. Also, using external heat flux can be improved nano-pumping mechanism time. It was expected that our designed system (CNT-C_{20} system) could be used in actual mass transfer applications.

Declaration of Competing Interest

The authors declare that they have no known competing financial interests or personal relationships that could have appeared to influence the work reported in this paper.

Data availability

No data was used for the research described in the article.

Acknowledgements

The authors extend their appreciation to the Deanship of Scientific Research at King Khalid University for funding this work through the large group Research Project under grant number RGP 2/247/44.

References

[1] Iijima S. Nature (London) 354 56 Crossref Google Scholar Ebbesen TW and Ajayan PM 1992. Nature (London) 1991;358:220.
[2] Iijima S. Helical microtubules of graphitic carbon. Nature 1991;354(6348):56–8.
[3] Endo M, Takeuchi K, Igarashi S, Kobori K, Shiraishi M, Kroto HW. The production and structure of pyrolytic carbon nanotubes (PCNTs). J Phys Chem Solid 1993;54 (12):1841–8.
[4] Yao Z, Postma HWC, Balents L, Dekker C. Carbon nanotube intramolecular junctions. Nature 1999;402(6759):273–6.
[5] Moniruzzaman M, Winey KI. Polymer nanocomposites containing carbon nanotubes. Macromolecules 2006;39(16):5194–205.
[6] S. Berber, and Y. Kwon, "Tom, aacute and D. nek.","*Unusually High Thermal Conductivity of Carbon Nanotubes*.
[7] Xu Z, Buehler MJ. Strain controlled thermomutability of single-walled carbon nanotubes. Nanotechnology 2009;20(18):185701.
[8] Mintmire JW, Dunlap BI, White CT. Are fullerene tubules metallic? Phys Rev Lett 1992;68(5):631.
[9] Tans SJ, Devoret MH, Dai H, Thess A, Smalley RE, Geerligs L, et al. Individual single-wall carbon nanotubes as quantum wires. Nature 1997;386(6624):474–7.
[10] Alam J, Riaz U, Ahmad S. Development of nanostructured polyaniline dispersed smart anticorrosive composite coatings. Polym Adv Technol 2008;19(7):882–8.
[11] Farzin A, Fathi M, Emadi R. Multifunctional magnetic nanostructured hardystonite scaffold for hyperthermia, drug delivery and tissue engineering applications. Mater Sci Eng C 2017;70:21–31.
[12] Wang J, Zhang Y, Liua G, Zhang T, Zhang C, Zhang Y, et al. Improvements in the Magnesium Ion Transport Properties of Graphene/CNT-wrapped TiO2-B Nanoflowers by Nickel Doping. Small 2023. https://doi.org/10.1002/smll.202304969.
[13] Karimzadeh S, Safaei B, Jen T-C. Theorical investigation of adsorption mechanism of doxorubicin anticancer drug on the pristine and functionalized single-walled carbon nanotube surface as a drug delivery vehicle: a DFT study. J Mol Liq 2021;322:114890.
[14] Naderi M, Karimipour A. Two-phase solid/liquid mixture of water/carbon nanotubes at the equilibration phase of atomic structures: atomic value effects in a microchannel using the molecular dynamics method. J Mol Liq 2021;339:116820.
[15] Vahedi A, Lahidjani MHS, Shakhesi S. Multiscale modeling of thermal conductivity of carbon nanotube epoxy nanocomposites. Phys B Condens Matter 2018;550:39–46.
[16] Safaei B, Naseradinmousavi P, Rahmani A. Development of an accurate molecular mechanics model for buckling behavior of multi-walled carbon nanotubes under axial compression. J Mol Graph Model 2016;65:43–60.
[17] von Ranke NL, Castro HC, Rodrigues CR. Molecular modelling and dynamics simulations of single-wall carbon nanotube as a drug carrier: new insights into the drug-loading process. J Mol Graph Model 2022;113:108145.
[18] Karimzadeh S, Safaei B, Jen T-C. Prediction effect of ethanol molecules on doxorubicin drug delivery using single-walled carbon nanotube carrier through POPC cell membrane. J Mol Liq 2021;330:115698.
[19] Pakdel M, Raissi H, Shahabi M. Predicting doxorubicin drug delivery by single-walled carbon nanotube through cell membrane in the absence and presence of nicotine molecules: a molecular dynamics simulation study. J Biomol Struct Dyn 2020;38(5):1488–98.
[20] Zhou X, Alizadeh A, Abd Alreda B, Fathdal F, Abbas JK, Albazoni HJ, Shamsborhan M, Nasajpour-Esfahani N, Hekmatifar M. The molecular dynamics description of electric field effect on nano-pumping performance of boron-nitride nanotube (BNNT) in the presence of vacancy defect. Colloids and Surfaces A: Physicochemical and Engineering Aspects 2023;666:131322.
[21] Xie Y, Al-Bahrani M, Nasajpour-Esfahani N, Jasim DJ, Hekmatifar M, Esmaeili S, et al. A computational study of the effect of external heat flux and electric field on the nano-pumping of C20 molecules in carbon nanotubes by molecular dynamics simulation. J Mater Res Technol 2023;25:1898–908.
[22] Weidong L, Al-Bahrani M, Alizadeh A, Nasajpour-Esfahani N, Shamsborhan M, Toghraie D. Variable electric field and atomic percentage of doping on the displacement process of C20 molecules in a nanotube with molecular dynamics simulation. TrAC Trends Anal Chem 2023:117210.
[23] Sabetvand R, Jami H. The study of boron-nitride nanotube behavior as an atomic nano-pump for biomedicine applications. J Mol Model 2022;28(1):19.
[24] Madani SZM, Safaee MM, Gravely M, Silva C, Kennedy S, Bothun GD, et al. Carbon nanotube–liposome complexes in hydrogels for controlled drug delivery via near-infrared laser stimulation. ACS Applied Nano Materials 2020;4(1):331–42.
[25] Zhang B, Hao M, Xiong J, Li X, Koopman J. Ab initio molecular dynamics calculations on electron ionization induced fragmentations of C4F7N and C5F10O for understanding their decompositions under discharge conditions. Phys Chem Chem Phys 2023;25(10):7540–9. https://doi.org/10.1039/D2CP03498K.
[26] Liu X, Ghafari B, Patra I, Kadhim MM, Turki Jalil A, Kumar Anil, et al. A molecular dynamics study of thermal behavior of ammonia/Cu nanorefrigerant flow under different initial pressures and electric fields. J Mol Liq 2022;367(120388):120388. https://doi.org/10.1016/j.molliq.2022.120388.
[27] Liu X, Patra I, Kuzichkin OR, Zaidi M, Abdulnabi SM, Mohsen Najm Z, et al. Molecular dynamics study of the effect of external electric field amplitude and cavity on thermal properties of Ammonia/Copper Nano-Refrigerant. J Mol Liq 2022;365(120125):120125. https://doi.org/10.1016/j.molliq.2022.120125.
[28] Liu X, Adibi M, Shahgholi M, Tlili I, Sajadi SM, Abdollahi A, et al. Phase change process in a porous carbon-paraffin matrix with different volume fractions of copper oxide nanoparticles: a molecular dynamics study. J Mol Liq 2022;366:120296.
[29] Li S, Sajadi SM, Alharbi KAM, El-Shorbagy M, Tlili I. The molecular dynamics study of vacancy defect influence on carbon nanotube performance as drug delivery system. Eng Anal Bound Elem 2022;143:109–23.
[30] Rapaport DC, Rapaport DCR. The art of molecular dynamics simulation. Cambridge University Press; 2004.
[31] Spreiter Q, Walter M. Classical molecular dynamics simulation with the Velocity Verlet algorithm at strong external magnetic fields. J Comput Phys 1999;152(1):102–19.
[32] Hairer E, Lubich C, Wanner G. Geometric numerical integration illustrated by the Störmer-Verlet method. Acta Numerica 2003;12:399–450.

[33] Toghraie D, Hekmatifar M, Salehipour Y, Afrand M. Molecular dynamics simulation of Couette and Poiseuille Water-Copper nanofluid flows in rough and smooth nanochannels with different roughness configurations. Chem Phys 2019; 527:110505.
[34] Daw MS, Baskes MI. Embedded-atom method: Derivation and application to impurities, surfaces, and other defects in metals. Phys Rev B 1984;29(12):6443.
[35] J. E. Lennard-Jones, "Cohesion," *Proceedings of the Physical Society (1926-1948)*, vol. 43, no. 5, pp. 461, 1931.
[36] Tersoff J. New empirical approach for the structure and energy of covalent systems. Phys Rev B 1988;37(12):6991.
[37] Rappé AK, Casewit CJ, Colwell K, Goddard III WA, Skiff WM. UFF, a full periodic table force field for molecular mechanics and molecular dynamics simulations. J Am Chem Soc 1992;114(25):10024–35.
[38] Mayo SL, Olafson BD, Goddard WA. DREIDING: a generic force field for molecular simulations. J Phys Chem 1990;94(26):8897–909.
[39] https://docs.lammps.org/compute_entropy_atom.html.
[40] Sawant SV, Patwardhan AW, Joshi JB, Dasgupta K. Boron doped carbon nanotubes: Synthesis, characterization and emerging applications–A review. Chem Eng J 2022;427:131616.